Spectroscopy of Sm^{145} via (d,p) Reactions

R. K. JOLLY* AND C. F. MOORE
Department of Physics, Florida State University, Tallahassee, Florida†
and
Department of Physics, University of Pittsburgh, Pittsburgh, Pennsylvania‡

(Received 19 August 1965; revised manuscript received 13 December 1965)

States of Sm^{145} have been investigated via 15-MeV–deuteron-induced (d,p) reactions with an energy resolution of ~40 KeV. The angular-distribution data have been analyzed using zero-range distorted-wave Born-approximation calculations to extract spectroscopic information. The proton spectra do not show the simple structure that one would expect from the conventional shell model for an 82-neutron target nucleus. Spin and parity assignments for most of the observed levels together with single-particle energies are presented.

I. INTRODUCTION

STRIPPING reactions on "magic"-neutron-number nuclei are very convenient for studying the neutron shell structure in view of the simplicity of the final-state neutron configurations. The proton groups from these reactions are well separated and rather few compared to those from neighboring isotopes.

Spectroscopy of Sm^{145} using the (d,p) reaction was done to study the $82<N\leqslant 126$ neutron shell structure. Previous work[1–3] on closed-shell nuclei of Ba^{138}, Ce^{140}, Pr^{141}, Nd^{142}, and Sm^{144} has been done to investigate this same region. We shall have occasion to refer to these experiments later in the present paper. In particular the energy levels of Sm^{145} have been measured by Kenefick[3] with an energy resolution of ~15 keV. However, in Kenefick's experiment no attempt was made to measure angular distributions. The present experiment was undertaken to supply these data in order to study more completely the level structure of Sm^{145} and compare the results with other 83-neutron nuclei.

II. EXPERIMENTAL PROCEDURE

15-MeV deuterons from the University of Pittsburgh cyclotron bombarded a target of Sm_2O_3 (Sm^{144} 95% and other isotopes less than 1%) prepared by electron-bombardment evaporation onto a carbon backing of thickness ~50 $\mu g/cm^2$. The reaction products were analyzed by a 60-deg wedge-magnet spectrograph and detected in nuclear-emulsion plates. Other details of the experimental method have been discussed elsewhere.[4]

The target thickness of samarium as measured by Rutherford scattering was ~0.85 mg/cm^2. However, this thickness may be somewhat in error since the target used in the present experiment was nonuniform (a circle of $\frac{1}{2}$-in. radius, thick at the center and thinner at the edge by a factor of 2) and the effective thickness at the beam spot ($\frac{1}{2}$ in.$\times\frac{1}{8}$ in.) may be different from the average thickness used in the present calculations.

With the exception of $i_{13/2}$, one expects to excite only odd-parity states of orbitals $1h$, $2f$, and $3p$ in the $82<N\leqslant 126$ neutron shell. For 15-MeV deuterons the (d,p) reaction studies of Fulmer *et al.*[2] on Ce^{140} and other 82-neutron nuclei showed that angular-distribution measurements between 10 and 60 deg were adequate to identify the angular momentum of the neutrons captured in the various shell-model states listed above. Consequently, proton spectra in the present experiment were recorded at 10, 15, 20, 27.5, 35, 42.5, 50, and 57.5 degrees.

III. DATA REDUCTION AND ANALYSIS

A typical energy spectrum of protons from the $Sm^{144}(d,p)Sm^{145}$ reaction observed at 42.5 deg is shown in Fig. 1. The "line" width at half-maximum is 41 keV, though at some other angles the energy resolution was slightly better than that observed here. The points shown in the figure are the number of proton tracks per 5 mm^2 of exposed area at $\frac{1}{2}$-mm intervals along the nuclear-emulsion plate. The smooth curve drawn through the experimental points is a least-squares fit to the data using a skew Gaussian for the intensity distribution of a single proton group. Exact intensity peak locations, needed in calculating the excitation energies of corresponding states of the residual nucleus, were determined using the above fitting procedure. The areas of isolated peaks were determined more accurately by actually counting all the proton tracks in each group.

The measured angular distributions were analyzed for orbital angular momentum (l_n) of the captured neutron by comparison with theoretical differential cross sections calculated using the zero-range distorted-wave Born-approximation (DWBA) theory without the spin-orbit interaction. The proton and deuteron optical-potential parameters were the average param-

* Present address: Atomic Energy Research Establishment, Harwell.

† Supported by the U. S. Air Force Office of Scientific Research.
‡ Supported by the National Science Foundation and the U. S. Office of Naval Research.

[1] G. B. Holm and H. J. Martin, Jr., Phys. Rev. **122**, 1537 (1961).
[2] R. H. Fulmer, A. L. McCarthy, and B. L. Cohen, Phys. Rev. **128**, 1302 (1962).
[3] R. A. Kenefick, Ph.D. thesis, Florida State University, 1962 (unpublished).
[4] B. L. Cohen, R. H. Fulmer, and A. L. McCarthy, Phys. Rev. **126**, 698 (1962).

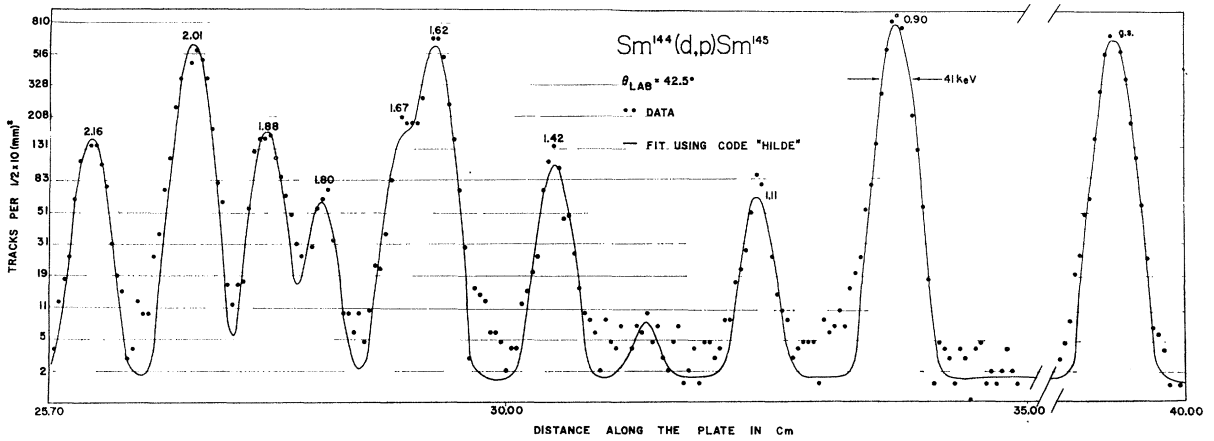

FIG. 1. Proton spectrum from the (d,p) reactions on Sm^{144} observed at 42.5°(lab). The points are a plot of intensity versus distance along the nuclear-emulsion plate and the smooth curve going through them is a least-squares fit to the spectrum with a skew Gaussian at each intensity peak location. The numbers appearing above the intensity peaks are excitation energies relative to the ground state (g.s.) of the residual nucleus.

eters of Perey and Perey[5] obtained from fitting extensive intermediate-energy proton and deuteron elastic-scattering data with a pure surface-absorption model. These parameters are listed in Table I.

Spin assignments to the states of Sm^{145} were made using: (i) the fact that the ground state of Sm^{144} is 0^+; (ii) the conventional shell-model ordering of states, viz., that $j=l+s$ member of the $\mathbf{l\cdot s}$ doublet lies lower in the potential well than the $j=l-s$ member; (iii) the approximate magnitude of the $\mathbf{l\cdot s}$ splitting obtained from Ref. 6 (See Table II); (iv) the sum rule, $\sum_m S_j{}^m=1$, for the spectroscopic factors $S_j{}^m$, for the various components (denoted by the superscript 'm') for each of the two single-particle states $j=l+s$ or $l-s$ for a certain l value. An estimate of the spreading width (ΔE) for the various components of a single-particle state may be made using the following result from the giant-resonance theory[4,7], i.e., $\Delta E \simeq \frac{2}{3}E^*$, where E^* is the excitation energy of the single-particle state in question.

The spectroscopic factors can be further used to determine the single-particle energies E_j. These are calculated as centers of gravity of the observed members of same spin and parity of a single-particle transition multiplet, viz.,

$$E_j=\sum_m E_j{}^m S_j{}^m / \sum_m S_j{}^m, \quad (1)$$

where $E_j{}^m$ are the excitation energies of the various states of the same spin and parity.

TABLE I. The parameters of the deuteron and proton optical potential used in the DWBA calculations of cross sections for the $Sm^{144}(d,p)Sm^{145}$ reactions. V and W are, respectively, the depths of the real and imaginary (surface absorption) potential well. r_0 and a are the radius and the diffuseness, respectively, of the real well, while the corresponding primed symbols are for the imaginary well. r_{0c} is the Coulomb radius constant. The imaginary well depth W here is 4 times that of Ref. 5.

	V (MeV)	r_0 (F)	a (F)	W (MeV)	r_0' (F)	a' (F)	r_{0c} (F)
15-MeV deuterons	104	1.15	0.81	58	1.34	0.60	1.3
17-MeV protons	52	1.25	0.64	67	1.25	0.47	1.25

IV. RESULTS AND DISCUSSION

A. Excitation Energies

The excitation energies of the various states observed in the present experiment are listed in Table III and compared with the measurements of Kenefick in Fig. 2. The agreement between the two sets of data is quite good, taking into account the energy resolution in the two experiments. It is obvious from this comparison that at higher excitation energies we have not been able to resolve some close doublets and triplets seen in the measurements of Kenefick.

B. Angular Distributions and Spin Assignments

The experimental angular distributions and their comparison with the DWBA predictions are shown in

TABLE II. $\mathbf{l\cdot s}$ splitting magnitudes for the shell-model states of Sm^{145}. l is the orbital angular momentum associated with a shell-model orbital.

l	$\mathbf{l\cdot s}$(MeV)
2	~2.0
4	~2.5
6	~5.5
1	~1.0
3	~1.8
5	~6.0

[5] C. M. Perey and F. G. Perey, Phys. Rev. **132**, 755 (1963); F. G. Perey, *ibid.* **131**, 745 (1963).

[6] B. L. Cohen, P. Mukherjee, R. H. Fulmer, and A. L. McCarthy, Phys. Rev. **127**, 1678 (1962).

[7] A. M. Lane, R. G. Thomas, and E. P. Wigner, Phys. Rev. **98**, 693 (1955).

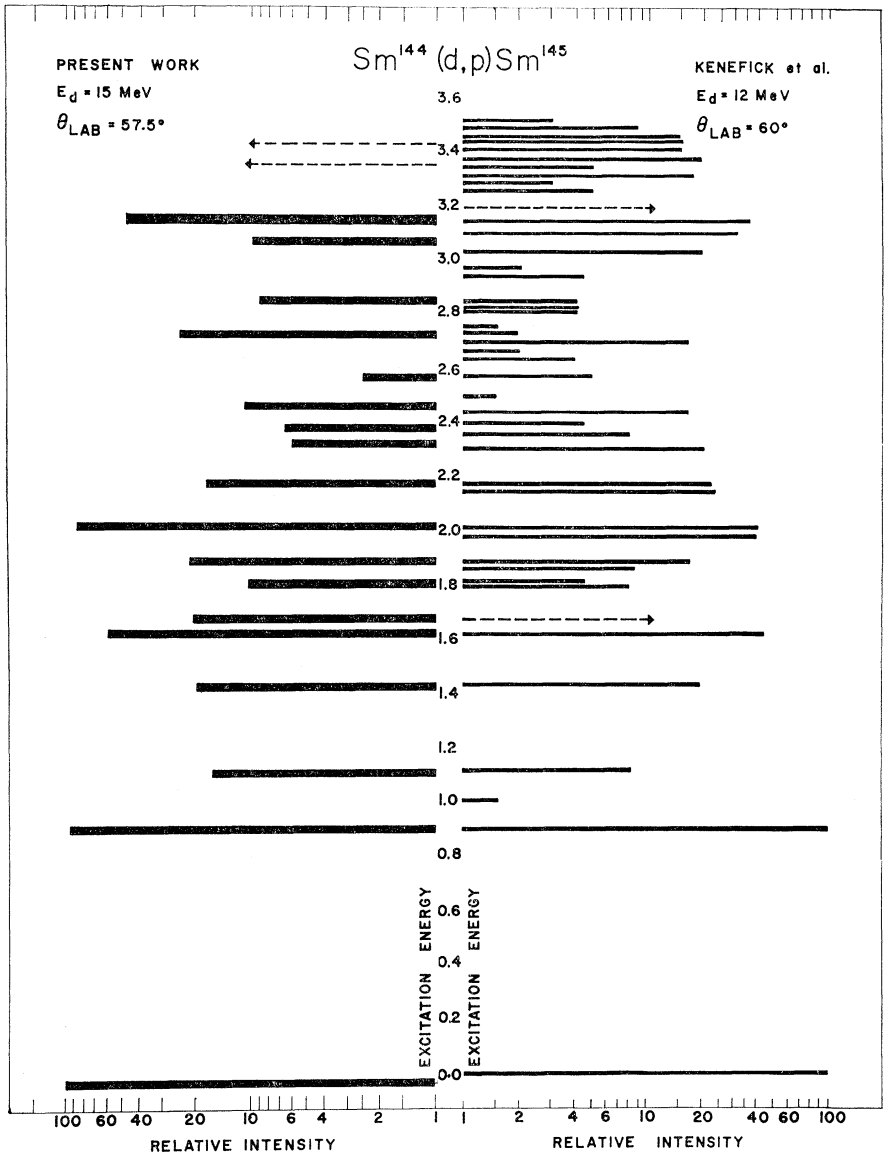

FIG. 2. A ("back-to-back") comparison of the energy spectra of protons from the $Sm^{144}(d,p)Sm^{145}$ reactions measured in the present work and Ref. 3. The excitation energy (in MeV) is plotted along the vertical axis (linear scale) while the relative intensities are plotted along the horizontal axis (logarithmic scale) making the intensities of the ground-state groups in the two measurements the same. The widths of the lines approximately correspond to the energy resolution in the two experiments.

Figs. 3, 4, and 5. The shape agreement between the data and the DWBA predictions (with no lower cutoff) in the case of the well-separated, and strongly excited, ground and the first excited state (0.90 MeV) is quite good. Encouraged by the success of the DWBA predictions for the above well-resolved groups, an attempt has been made in the case of unresolved doublets to simulate their angular distributions by suitable linear combinations of the DWBA cross sections for the possible l values corresponding to the unresolved groups. It may be remarked here that for the first few MeV of excitation energy above the ground state in Sm^{145} one expects to see only the odd $-l$ states. This may be seen from the magnitudes of the various $\mathbf{l}\cdot\mathbf{s}$ doublet splittings listed in Table II. The separation between the consecutive major shells is $\sim$8 MeV, while the spreading of the $g(l=4)$ and the $d(l=2)$ single-particle states around their centers of gravity would be $\sim\pm 2$ MeV. This indicates that few even-parity states, except $i_{13/2}$, will be excited with an appreciable cross section below 5–6 MeV of excitation energy in the case of Sm^{145}. Since states only up to 3.5 MeV of excitation energy were investigated in the present work, for the purpose of analyzing angular distributions of unresolved doublets, the presence of only odd parity (p, f, and h) states was assumed on the basis of the foregoing arguments. Further, the authors did not notice any evidence for any even parity state in this work.

Examples of the above procedure of simulating the measured angular distributions of unresolved doublets by taking appropriate linear combinations of DWBA cross sections for admissible l values, are provided by

the data for the 1.11-MeV (Fig. 5) and the 2.44-MeV (Fig. 4) groups. However, the spectroscopic factors extracted by this procedure are not sometimes very reliable for the following reason. On account of the finite size of the error bars in the experimental data there exists a continuous range of coefficients for the aforesaid linear combinations of DWBA cross sections that can be used with equal validity to simulate the observed angular distributions of unresolved doublets.

An interesting feature of the DWBA calculations used here is the fact that, contrary to the experience in other heavy nuclei,[8] the experimental data in the present work best agree with calculations done without any lower cutoff. This point is illustrated in Fig. 6. Although the preference for zero lower cutoff is not so clear for $l=1$, it is unmistakable in the $l=3$ case. For the $l=5$ case (not shown in Fig. 6), all predictions agree poorly with the data but again it is the zero-lower-cutoff calculation that comes closest to the experiment. The spectroscopic factors listed in Table III have been calculated from a zero-lower-cutoff prediction. For $l=1$ and $Q=4.6$ MeV the spectroscopic factors for a lower cutoff of 8.8 F are too large by ~25%. A similar calculation for $l=3$ yields spectroscopic factors that are five times too large at angles $<15°$ and ~50% too large between 20° and 40°. This large variation in the spectroscopic factor with angle is on account of the change in shape of the predicted (DWBA) angular distribution as one changes the lower cutoff. The situation with regard to the effect of lower cutoff on spectroscopic factors for $l=5$ is similar to that for $l=3$. It is quite likely that the lower cutoff that best describes our data is not exactly zero but rather small. Further the optical-potential parameters employed in the calculations used here are average parameters and a slight change in the parameters of the absorptive well can perhaps account for the effect of the presence or absence of a small lower cutoff. An upper cutoff of three times the nuclear radius was employed in all calculations used in this work. This seems quite satisfactory here, although for small l_n and Q values, a higher upper cutoff and a correspondingly larger number of partial waves are recommended.[9]

Another notable feature of the angular distributions is that they are quite different for different l_n values despite the rather large Coulomb barrier (12 MeV) for Sm^{144}.

The results of the various analyses outlined above and in the preceding section are presented in Table III.

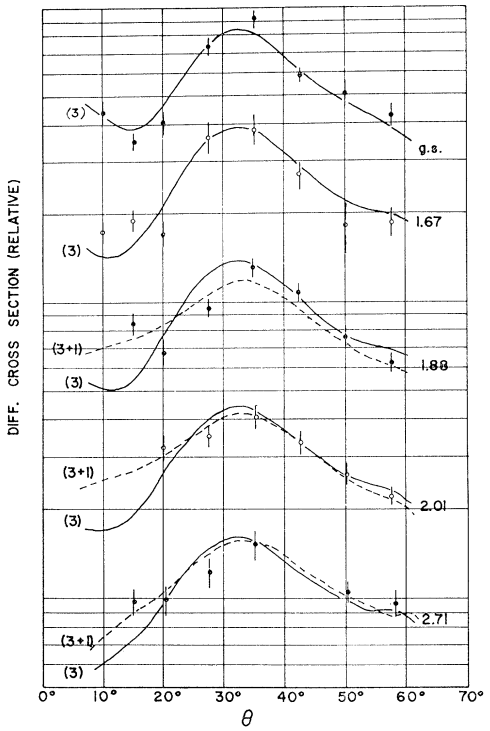

FIG. 3. Angular distributions of the proton groups leading to some $2f$ states of Sm^{145}. The curves going through the experimental points are the DWBA calculations. The numbers on the left of the angular distributions are the orbital angular momenta of the captured neutron while those on the right are excitation energies in MeV. In some cases a suitable linear combination (broken curves) of the DWBA cross sections for different angular momenta had to be taken to fit the experimental angular distribution. This is indicated by putting a plus sign between the orbital angular momenta noted within parentheses. (g.s.=ground state.)

TABLE III. Spectroscopic data from the analysis of $Sm^{144}(d,p)$-Sm^{145} reactions. Parenthesis indicate probability rather than certainty. Bracketed rows refer to an unresolved group of states whose angular distribution has been simulated with a suitable linear combination of DWBA cross sections for the values of angular momenta of the captured neutron (l_n) indicated in the appropriate column in the table. Other details may be found in the text.

Excitation energy (MeV)	l_n	J^π	$d\sigma/d\Omega(35°)$ [mb/sr]	$S_j{}^m$
g.s.	3	$\frac{7}{2}^-$	2.69	0.58
0.90	1	$\frac{3}{2}^-$	2.30	0.34
1.11	(5)	$\frac{9}{2}^-$	0.11	0.25
1.42	(5+1)	$\frac{9}{2}^-$, $\frac{3}{2}^-$	0.23 {0.13, 0.10}	{0.25, 0.015}
1.62	1	$\frac{3}{2}^-$	1.47	0.20
1.67	3	$\frac{5}{2}^-$	0.49	0.11
1.80	(5+1)	$\frac{9}{2}^-$, $\frac{3}{2}^-$	0.10 {0.05, 0.05}	{0.11, 0.007}
1.88	(3)	$\frac{5}{2}^-$	0.49	0.10
2.01	(3)	$\frac{5}{2}^-$	1.68	0.34
2.16	(1)	$\frac{1}{2}^-$	0.40	0.10
2.31	...	...	0.11	...
2.37	...	...	0.13	...
2.44	(1+3)	$\frac{1}{2}^-$, $\frac{5}{2}^-$	0.27 {0.09, 0.18}	{0.043, 0.017}
2.56	...	...	0.06	...
2.71	(3)	$\frac{5}{2}^-$	0.43	0.076
2.84	...	...	0.17	...
3.06	...	...	0.18	...
3.14	(1)	$\frac{1}{2}^-$	0.88	0.18
3.35	...	...	0.27	...
3.45	(1)	$\frac{1}{2}^-$	0.92	0.18

[8] E. J. Schneid, A. Prakash, and B. L. Cohen (to be published); R. K. Jolly, Phys. Rev. **136**, B683 (1964).

[9] G. R. Satchler (private communication).

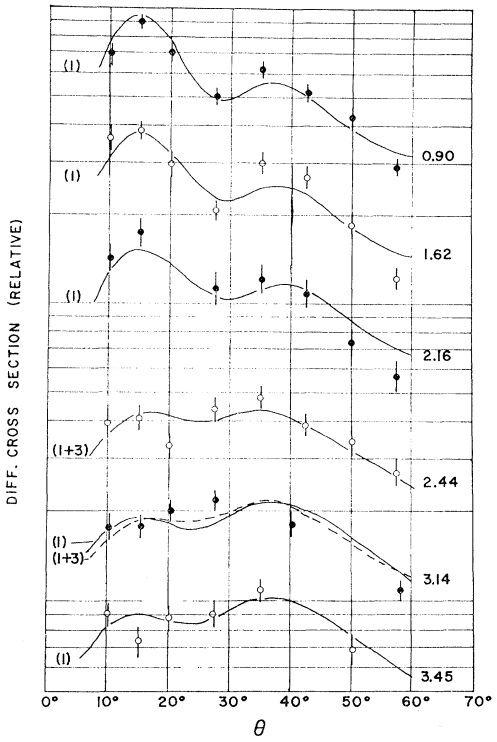

FIG. 4. Angular distributions of the proton groups leading to various $3p$ states in Sm^{145}. See also the caption for Fig. 3.

For the purpose of discussion, the various angular distributions have been classified below according to the angular momentum of the captured neutron and are accordingly distributed among Figs. 3, 4, and 5.

Figure 3 shows the experimental angular distributions and their comparison with the DWBA predictions (solid and broken curves) for the ground state (g.s.), the 1.67-, 1.88-, 2.01-, and 2.71-MeV groups. The angular distributions for the ground state and the 1.67-MeV groups agree very well in shape with the DWBA curves for a neutron capture into a $2f$ shell model state. The 1.88-MeV group seems to be a doublet both from its width and comparison with the better resolution data of Kenefick (Fig. 2). Except for the 15° point, its angular distribution agrees with the DWBA prediction for $l_n=3$ (solid curve). However, if the weaker of the two unresolved groups corresponds to a $3p$ capture, the predicted angular distribution can be changed to the shape of the broken curve. The difference between the two curves is probably not very significant. Since the $l_n=3$ component is dominant, we list only that in Table III. The situation for the 2.01- and 2.71-MeV groups is similar to that for the 1.88-MeV group. However, in the case of the 2.01-MeV group the two unresolved components, (Fig. 2) are equally intense and their cross sections are rather large. The choice between the two possibilities $l=1$ or $l=1+3$ was made using the sum rule $\sum_m S_j{}^m=1$ and a comparison with the neutron single-particle energies for other 83 neutron nuclei from the work of Fulmer *et al.* A discussion of these is presented below in Sec. IV.C.

Figure 4 presents the experimental angular distributions for the 0.90-, 1.62-, 2.16-, 2.44-, 3.14-, and 3.45-MeV groups. The agreement of the angular distributions with the DWBA predictions for $l_n=1$ is quite good for the first three groups. The angular distribution for the 2.16-MeV group, a doublet comprising two equally intense components, corresponds to an $l_n=1$ capture for both members. The data for the 2.44-MeV group is best reproduced by a linear combination of DWBA cross sections for $2f$ and $3p$ capture. The seeming isotropy of the 2.44-MeV group is owing to the different (somewhat out of phase at small angles) angular distributions of the unresolved components. It is further aggravated by the fact that the angular distributions lose their structure (peak-to-valley ratio decreases) as one goes to smaller Q values (e.g., compare the predictions for the 0.90- and the 3.45-MeV groups in Fig. 4).

The experimental data for the 3.14- and 3.45-MeV groups (which are definitely multiple both from an examination of their widths and Fig. 2) agree with the DWBA curves for $l_n=1$. However, a small admixture of an $l_n=3$ cross section does not seem to alter the slowly varying shape of the angular distribution (see the broken curve for the 3.14-MeV group). Only $l_n=1$ has been listed in Table III for the above two groups.

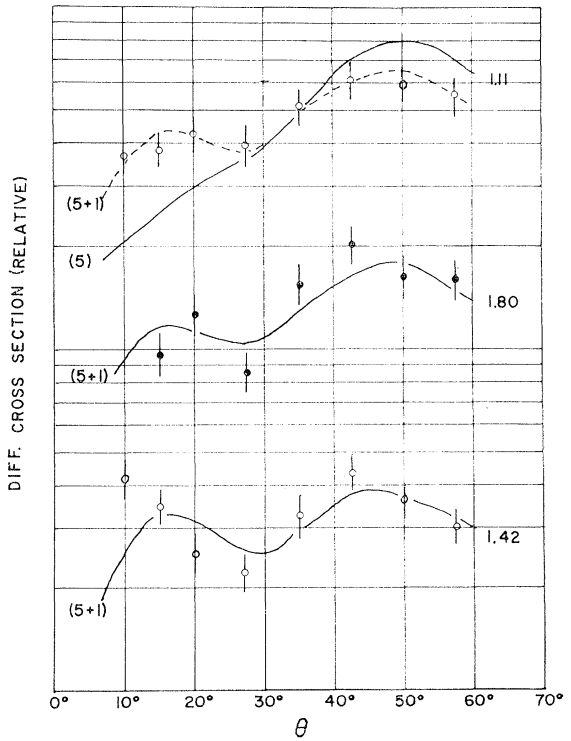

FIG. 5. Angular distributions of the proton groups leading to the various $1h_{9/2}$ states in Sm^{145}. See also the caption for Fig. 3.

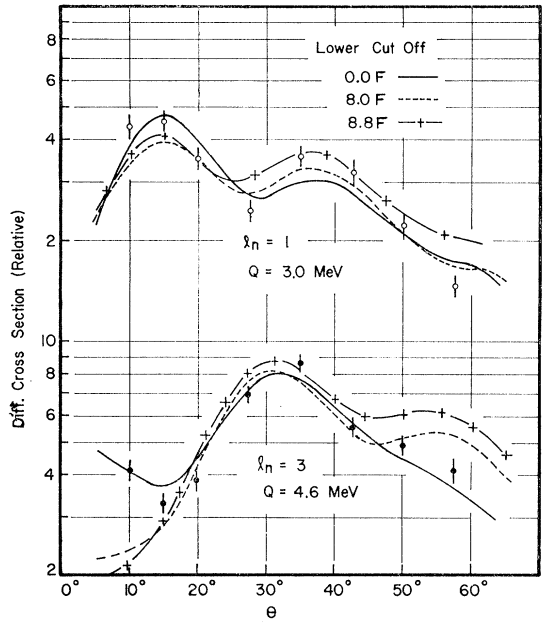

FIG. 6. A comparison of the DWBA predictions for $l_n=1$ and 3 and for different lower cutoffs with the experimental angular distributions (open and solid circles). The various DWBA curves have been adjusted arbitrarily for a best visual fit to the data.

The angular distributions for the 2.31- and 2.37-MeV groups have not been presented because of large uncertainties in their rather low cross sections. Nevertheless, the data for the former group are evenly distributed about the theoretical curve for $l_n=1$ while that for the latter group can be simulated by a linear combination of $l_n=1$ and 3 cross sections.

The angular distributions for the 1.11-, 1.42-, and 1.80-MeV groups are shown in Fig. 5. These angular distributions all show a characteristic maximum between 40 and 50 deg. A comparison of the experimental curves and the DWBA calculations shows the closest agreement for $l_n=5$. The DWBA predictions for $l_n=5$ show a rather broad maximum at ~50 deg quite similar to the one that the data exhibit. This broad maximum does not leave any ambiguity with regard to the l-value assignment since the curves for $l=3$ and 6 are completely different from the experimental angular distributions for the above three groups. Although DWBA calculations for $l_n=5$ for the above three groups do not seem to be as successful (the solid curve for the 1.11-MeV group) as those for $l_n=1$ and $l_n=3$ discussed in the preceding paragraphs, it is felt that these groups are populated primarily by $l_n=5$ capture leading to $h_{9/2}$ states in Sm^{145}. The work of Fulmer *et al.* lends support to this conclusion in that they find some $h_{9/2}$ states in other 83-neutron nuclei in the same region of excitation energy (see Fig. 6).

The reasons for the poor agreement between the $l_n=5$ DWBA calculations and the experimental data in Fig. 5 are not certain. Since the $l_n=1$ and $l_n=3$ calculations have been very successful, there is no reason to suspect the calculations for $l_n=5$ to be in error. The slight disagreement between data for the 1.80-MeV group and DWBA calculations for $l_n=5$ may have a simple explanation in the fact that the measurements of Kenefick show a doublet at the same excitation energy. The experimental angular distribution for this group is simulated quite well by a linear combination of cross sections for $l_n=5$ and 1. Similar linear combinations of DWBA cross sections reproduce the data for the 1.11- and 1.42-MeV groups. However, there is no evidence of any doublets or multiplets in Ref. 3 for the case of the latter two groups. The 1.11-MeV group has a low cross section and, if one were to believe the validity of DWBA calculations for $l_n=5$, the presence of a very weak unresolved $l_n=1$ group from an isotopic impurity could explain the observed result. The contribution of $l_n=1$ in the 1.42-MeV group is quite appreciable and it is very probable that the $l_n=1$ group also belongs to the main isotope (Sm^{144}) in the target and is unresolved even in the better resolution measurements of Kenefick. The preceding conclusions with regard to the 1.11- and 1.42-MeV groups are, however, purely speculative and based only on a faith in the correctness of $l_n=5$ DWBA calculations.

It may be remarked that the curves for a linear combination of DWBA cross sections for $l_n=1$ and 5 do not seem very different from the curves for some combinations for $l_n=1$ and 6. However, it is expected that only one $l_n=6$ group will be seen in the observed spectra since there is no other even parity state in the $82<N\leqslant 126$ neutron shell. The DWBA prediction for $l_n=6$ shows a rather broad maximum centered at ~60° whereas all the angular distributions in Fig. 5 show a maximum between 40° and 50°. Probably none of the above three groups have an $l_n=6$ component although the possibility of its presence cannot be completely ruled out.

The angular distributions of the remaining groups listed in Table III are very uncertain and inconclusive. Of these the 3.06-MeV group seems to be single, judging from the data of Kenefick. Its angular distribution has a rather few points showing some resemblance to the DWBA curve for $l_n=1$.

The l value and spin assignments in Table III have been made using the procedures outlined above. Parentheses around assignments indicate probability rather than certainty. The ground-state spin is already known[10] to be $\frac{7}{2}^-$. The isobaric analogs of the ground state and the 0.90-, 1.62-, and 1.67-MeV states have been observed in elastic proton scattering experiments[11] and the l values from these experiments agree with those reported in the present paper. There is, however, some uncertainty in deciding the spins of the p states between 2.0 and 2.6 MeV of excitation energy. An extension of

[10] *Nuclear Data Sheets*, compiled by K. Way *et al.* (Printing and Publishing Office, National Academy of Sciences–National Research Council, Washington 25, D. C.)

[11] C. F. Moore and R. K. Jolly, Phys. Letters **19**, 139 (1965).

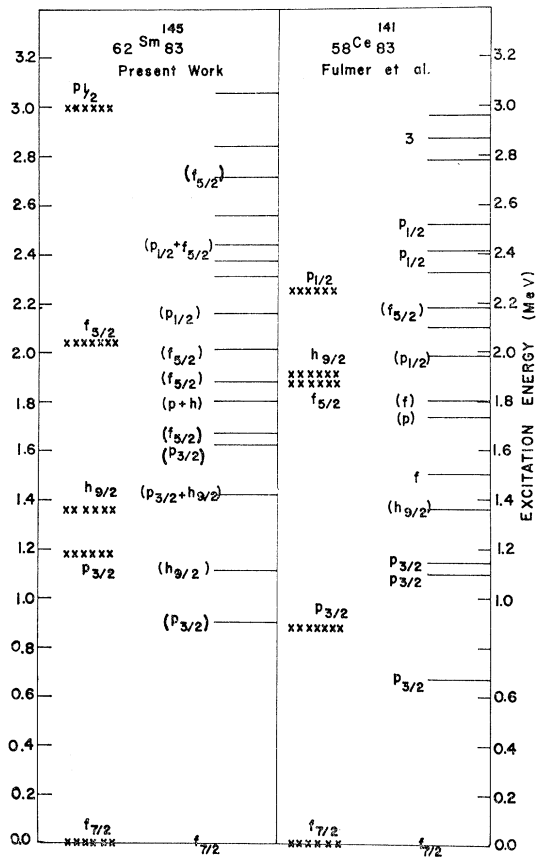

FIG. 7. A comparison of the low-lying energy levels of 83-neutron nuclei of Sm^{145} and Ce^{141}. Parentheses around assignments indicate probability rather than certainty. The locations of the center of gravity of the observed states of same spin and parity are shown by a row of X's. See Sec. IV for a discussion of the difference between the level spectra of the two isotonic nuclei.

the measured angular distributions to large angles probably could have resolved this ambiguity[12] but was found impractical for the experimental arrangement used in the present work. Nevertheless, the assignments listed in Table III were decided on the ground that they yield: (i) reasonable values of $\sum_m S_j{}^m$ for $\frac{1}{2}^-$ and $\frac{3}{2}^-$ states and (ii) a better agreement between the single-particle energies (see discussion below) calculated in this work and the work on other 82-neutron nuclei by Fulmer *et al.*[2]

C. Sum Rule and Single-Particle Energies

The single-particle energies and the corresponding values of $\sum_m S_j{}^m$ are listed in Table IV. The values of $\sum_m S_j{}^m$ for the various single-particle states are all too low by a factor of 1.6. The low values of $\sum_m S_j{}^m$ can result from uncertainties either in the magnitudes of the DWBA cross section or the target thickness or both. Since the shapes of the DWBA cross sections for $l_n=1$ and 3 agree very well with the experimental angular distributions, the spectroscopic factors obtained from the above comparison are expected to be quite correct. However, the target thickness may be somewhat in error as previously discussed in Sec. II.

The single-particle energies E_j's have been compared with those obtained by Fulmer *et al.*[2] from their work on other 82-neutron nuclei. The agreement is encouraging except in the case of the $h_{9/2}$ and $p_{1/2}$ states. The disagreement in the case of the $h_{9/2}$ may be due to large uncertainties in the spectroscopic factors for the various $h_{9/2}$ components since the cross sections for these states are usually small and the problem is further complicated if all of these groups are not resolved from other nearby groups. The low value of Fulmer *et al.* for $E_{1/2^-}$ could result from their having missed some $\frac{1}{2}^-$ components at higher excitation energies. This is quite reasonable as, in spite of the fact that the energy spectra in the present work have been analyzed for an MeV or so farther than in the work of Fulmer *et al.*, the value of $\sum_m S_{1/2^-}{}^m$ obtained here still seems relatively low indicating that some $\frac{1}{2}^-$ components at higher excitation energies may have been missed.

D. Summary of Results

Figure 6 summarizes the results of the present work and compares them with those of Fulmer *et al.* on the isotonic nucleus of Ce^{141}. Cerium has 4 protons less than Sm, and it is obvious that these 4 protons (filling the even parity $50<N\leqslant 82$ shell) make an appreciable difference in the level structure of the 83rd neutron. This is, however, only another addition to the already well-known result that, contrary to the expectation of the pairing theory, the addition of an even number of protons appreciably alters the level spectrum of the odd neutron in an odd-A nucleus.

An interesting feature of the spectrum of the 83rd neutron in Sm^{145} (or Ce^{141}) is that its structure is not as simple as one would expect from a closed-shell-plus-a-neutron model of such a nucleus. In Sm^{145} one can see from Table III that there are several states of the same spin and parity having rather comparable cross sections, indicating a fair amount of final-state configuration mixing.

TABLE IV. Values of E_j and $\Sigma_m S_j{}^m$ for Sm^{145}. The meaning of various symbols has been explained in the text. All energies are in MeV. A discussion of the consistently too low values of $\Sigma_m S_j{}^m$ may be found in Sec. IV.

Single-particle state	$\Sigma_m S_j{}^m$	E_j Present work	E_j Ref. 2
$f_{7/2}$	0.58	0.00	0.00
$p_{3/2}$	0.57	0.18	0.83
$h_{9/2}$	0.61	1.36	1.90
$f_{5/2}$	0.64	2.04	1.88
$p_{1/2}$	0.50	3.00	2.25

[12] L. L. Lee, Jr., and J. P. Schiffer, Phys. Rev. 135, B52 (1964).

ACKNOWLEDGMENTS

The authors are deeply indebted to Professor B. L. Cohen for permitting them to use the University of Pittsburgh cyclotron for taking the data reported in this work. Thanks are also due to Professor R. M. Drisko for his help in doing the DWBA calculations. The authors are grateful to Professor J. D. Fox for a thorough review of the final manuscript. They sincerely appreciate the support and encouragement of Professor R. H. Davis. The authors feel particularly indebted to Mrs. Meyers and collaborators for a very careful scanning of the nuclear-emulsion plates. The patient help of the secretarial staff of the Tandem Van de Graaff Accelerator Program is sincerely appreciated. Some of the DWBA calculations used in the present work were performed at the computing center of the University of Pittsburgh, which is partially supported by the National Science Foundation (Grant No. G-11309).

PHYSICAL REVIEW VOLUME 145, NUMBER 3 20 MAY 1966

New Type of Accelerator for Heavy Ions*

G. S. JANES, R. H. LEVY, H. A. BETHE,† AND B. T. FELD‡
Avco-Everett Research Laboratory, Everett, Massachusetts
(Received 10 December 1965)

A new device, called the heavy ion plasma accelerator (HIPAC), which may be capable of accelerating ions of any atomic number to energies sufficient to overcome the nuclear Coulomb barrier, is described. A closed potential well is created by filling a toroidal vacuum chamber with electrons; the electrons are contained by a magnetic field whose intensity is so low that its effect on the ions can be neglected. Ions are both accelerated and trapped in the well; the trapping effect allows sufficient time for the ions to become highly stripped by electron impact. The very large ion energies that can be achieved in this way would allow a wide variety of nuclear reactions to be studied, including inverse fission. The present primitive state of development of the HIPAC is described, and the future prospects assessed.

I. INTRODUCTION

A NEW device, called the heavy ion plasma accelerator (HIPAC), is suggested which may make possible the performance of presently unattainable experiments involving nuclear and energetic atomic reactions between heavy ions. Based on small scale experiments[1,2] and theoretical[3,4] work already performed, the outlook for the ultimate construction of the HIPAC is favorable, but there are nevertheless important unanswered questions having to do with the attainment of useful operating conditions.

In outline, the HIPAC utilizes the potential well due to a cloud of electrons; the electron cloud is established and controlled through the use of time-varying magnetic fields. The potential well serves the dual function of accelerating and trapping heavy ions that may be introduced, while the electrons of the cloud produce a high degree of stripping of these ions. Since the ion energy is proportional to the charge state as well as to the well depth, a well depth of 20 million volts would create center-of-mass energies sufficient to overcome the Coulomb barrier for collisions between nuclei of all species (see Fig. 1). For the heavy elements ($Z \geq 20$) this condition cannot be matched by any presently existing or proposed device. Well depths such as this, while representing an extrapolation on present achievements, appear nevertheless to be accessible in apparatus of relatively modest dimensions and cost. If they can indeed be reached, a considerable range of experiments involving nuclear reactions between heavy elements becomes accessible. Thus, for example, collisions between like or unlike nuclei of atomic number in the medium range 30–50 should give rise to the inverse of the nuclear-fission process. Studies of inverse fission could cast important new light on the dynamics of the fission process. While available "heavy" ion accelerators have already uncovered an interesting variety of new interactions, they have only scratched the surface of the possibilities which should be available to the HIPAC for which there are no inherent limitations on the nuclei available for study. Reactions between complex nuclei are presently achieved[5] by accelerating projectiles in a

* This work has been supported by the U. S. Air Force Office of Scientific Research of the Office of Aerospace Research, U. S. Air Force under Contract No. AF49(638)-1553.

† Permanent address: Cornell University, Ithaca, New York.

‡ Permanent address: Massachusetts Institute of Technology, Cambridge, Massachusetts.

[1] G. S. Janes, Phys. Rev. Letters **15**, 135 (1965).

[2] G. S. Janes, R. H. Levy, and G. E. Cooper, Bull. Am. Phys. Soc. **11** (1966) (to be published).

[3] R. H. Levy, Phys. Fluids **8**, 1288 (1965).

[4] O. Buneman, R. H. Levy, and L. M. Linson, J. Appl. Phys. (to be published).

[5] E. L. Hubbard, Ann. Rev. Nucl. Sci. **11**, 419 (1961).